In situ Adhesion Measurements Utilizing Layer-by-Layer Functionalized Surfaces

Adam J. Nolte,[†] Jun Young Chung,[†] Marlon L. Walker,[‡] and Christopher M. Stafford*[,†]

Polymers Division and Surface and Microanalysis Science Division, National Institute of Standards and Technology, 100 Bureau Drive, Gaithersburg, Maryland 20899

ABSTRACT The adhesion between poly(dimethylsiloxane) (PDMS) hemispheres coated with layer-by-layer (LbL) assemblies of polyelectrolytes and rigid, planar substrates was investigated using Johnson, Kendall, and Roberts (JKR) contact mechanics. Measurements were performed against amine-functionalized glass slides both in air and in aqueous solutions of controlled pH. Despite the increased density of negatively charged carboxylate groups, LbL-functionalized PDMS exhibited lower adhesion because of the combined effects of increased surface roughness and the high Young's modulus of the coating. Measurements of coated PDMS in aqueous solutions revealed tunable adhesion behavior dominated by pH-mediated changes in the mechanical properties of the coating. Smoothing the surface of the LbL coatings by aqueous salt annealing led to a significant increase in adhesion. Our results suggest that LbL assembly can be an effective means of surface functionalization for in situ adhesion measurements, but understanding and predicting the adhesion behavior requires comprehensive knowledge of the chemical, mechanical, and topological properties of the coating and how such properties change in response to the ambient environment.

KEYWORDS: JKR • adhesion • layer-by-layer • polyelectrolyte • responsive • contact mechanics • roughness

INTRODUCTION

Adhesion at polymer interfaces is a topic of great technological importance in a number of fields where the ability to accurately measure how well surfaces adhere could provide an indicator of device performance or serve as an effective screening tool. Recent advances in organic electronics, for example, have demonstrated a positive correlation between adhesion and device efficiency at polymer-electrode interfaces (1), and combinatorial studies involving adhesion measurements have been shown to be reliable methods of screening protein adsorption to various polymer blends (2). Regardless of application, a successful metrology for polymer adhesion must incorporate not only versatility in the composition of the contacting surfaces but also control of the measurement environment, as ambient conditions play an active role in governing interfacial molecular interactions.

In response to these and other challenges, adhesion measurement techniques such as functionalized-tip atomic force microscopy (AFM) (3) and the surface forces apparatus (SFA) (4) have been developed. Although both techniques are capable of measuring extremely small forces with good accuracy, practical limitations such as instrument cost, small contact area size (AFM), the need for extremely smooth surfaces (SFA), and the challenge of surface functionalization for both devices narrow their range of practical use. Nevertheless, a measurement platform capable of sensitive and straightforward adhesion measurements on an array of surface types could have a number of applications in both research and industrial environments. In this paper, we report our efforts to develop such a measurement platform utilizing the contact mechanics theory of Johnson, Kendall, and Roberts (JKR) (5).

JKR measurements of adhesion generally involve bringing an elastic, hemispherical probe (lens) with radius of curvature R into contact with an opposing rigid, planar substrate (Figure 1a). During the course of the measurement, the lens is pushed into the substrate (loading segment) until the force reaches a predetermined maximum value, after which it is withdrawn from the substrate (unloading segment) until detachment occurs. By tracking the load (P) and radius of the circular contact area (a) during the test, one can solve for both the plane-strain Young's modulus of the lens (E^*) and the energy release rate (G), which is the net change in interfacial energy associated with increasing or decreasing the contact area between the lens and substrate

$$G = \frac{\left(\frac{4E^*a^3}{3R} - P\right)^2}{8\pi E^* a^3} \quad (1)$$

Higher values of G are often measured during the unloading portion of the experiment, analogous to the differences observed between advancing and receding contact angle measurements. It is often assumed that the average value of G on loading (G_L) provides the closest estimate of the thermodynamic work of adhesion (W), whereas the relatively higher average G obtained on unloading (G_{UL}) reflects interfacial restructuring and bond formation between the surfaces in contact. Nevertheless, some authors have pointed out that G_L does not always match the predicted W from contact angle analysis (6) and that G_{UL} can be strongly rate-

* To whom correspondence should be addressed. E-mail: chris.stafford@nist.gov.

Received for review September 29, 2008 and accepted November 30, 2008

[†] Polymers Division, National Institute of Standards and Technology.

[‡] Surface and Microanalysis Science Division, National Institute of Standards and Technology.

DOI: 10.1021/am8000874

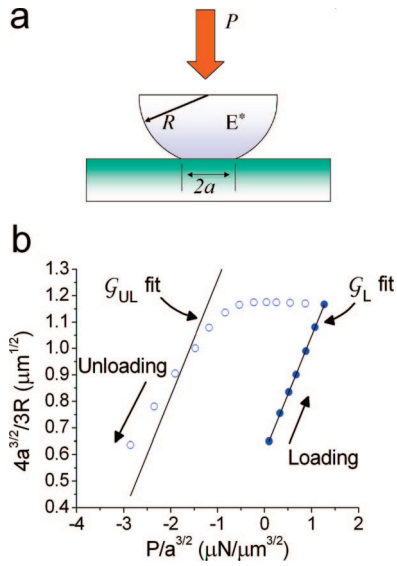

FIGURE 1. (a) Side-view schematic of an elastic lens contacting a rigid substrate during a JKR adhesion test. (b) Plots of loading (●) and unloading (○) data using a linearized form of eq 1 allow calculation of the energy release rate on loading (G_L) and unloading (G_{UL}). The unloading portion of the experiment typically gives higher values of G than the loading portion because of interfacial restructuring within the contact zone and dissipative loss processes. A more detailed explanation of the data analysis is given in the Experimental Section. The data in (b) are for illustrative purposes only.

dependent and involve substantial dissipative loss processes along the circular contact perimeter and within the lens bulk for viscoelastic materials (7). In this work, we have attempted to minimize dissipative losses by conducting experiments in a quasi-static manner using highly elastic poly(dimethylsiloxane) (PDMS) as the lens material. To characterize the adhesion strength between surfaces, we have chosen to use the adhesion hysteresis, defined as $G_{HYS} = G_{UL} - G_L$. This parameter is thought to provide the best estimate of specific molecular interactions and bonding events that arise upon contact of the surfaces (8); thus, it was assumed to be the best figure of merit for determining the number of acid−base interactions (see below) that occur upon contact of the functionalized PDMS lens with the substrate.

Although PDMS is often chosen as the ideal lens material because of its ease of use, highly elastic mechanical response, and modulus tunability, it is difficult to chemically functionalize without resorting to techniques such as UV-ozonolysis (UVO), which can unpredictably alter the mechanical properties and roughness of the surface (9). Consequently, some researchers have simply opted to utilize the material of interest as the lens in the JKR experiment. This has been demonstrated, for example, with pH-sensitive hydrogels (10), and even living cells (11). These approaches are intriguing but limited to materials in ample supply that can form elastic networks—also, the JKR theory typically does not accurately describe the mechanics of cells and other vesicular structures (12, 13). Direct adsorption from solution and Langmuir−Blodgett (LB) techniques have been used by Dillow et al. (8) and Rundlöf et al. (14) to deposit receptor proteins and cellulose, respectively, onto PDMS surfaces for use in JKR tests. Such techniques, while permitting full control of the lens elasticity and using only small amounts of the material being investigated, still require amenable species with potentially uncertain adhesion to the PDMS.

In light of the above considerations, we have chosen to utilize conformal coatings created by layer-by-layer (LbL) assemblies of polyelectrolytes to chemically functionalize the PDMS lens surface. These coatings, created via alternating adsorption of positively and negatively charged polyelectrolyte species from solution, introduce a thin (in this study, ∼16−40 nm) surface layer with mechanical, topological, and chemical attributes dissimilar from the bulk PDMS lens material. LbL assembly is a flexible technique capable of incorporating a wide variety of macromolecular materials for which measurements of surface interactions could be of enormous scientific and technical interest; for example, coatings comprising various polyacids, polybases, colloids, DNA, and proteins have all been demonstrated (15−18). The ability to precisely control the composition and properties of the resulting coatings makes LbL assembly an attractive technique for modifying the adhesion properties of surfaces. Although LbL-assembled polyelectrolyte species have been employed by various researchers using AFM and SFA methods, this work is the first to our knowledge to utilize LbL coatings in a JKR-type experiment.

We chose to examine in situ acid−base adhesion interactions between PDMS lenses coated with carboxylic acid (COOH)-containing LbL assemblies and amine-functionalized (NH_2) glass substrates. We have used this system as a model to explore how a broad array of factors such as surface roughness, thickness, mechanical properties, and solution pH affect adhesion when LbL coatings are used as adhesion modifiers in JKR tests. Because of the flexibility of the LbL technique, our results should be broadly applicable to the study of adhesion interactions in other types of systems as well.

EXPERIMENTAL SECTION

Equipment and instruments or materials are identified in this work in order to adequately specify the experimental details. Such identification does not imply recommendation by the National Institute of Standards and Technology (NIST), nor does it imply that the materials are necessarily the best available for the purpose.

Molds for PDMS lenses were created using 1 cm diameter glass hemispherical lenses (Edmund Optics) and Norland Optical Adhesive 81 (Norland Products). Sylgard 184 PDMS (Dow Corning) was mixed according to the manufacturer's instructions and degassed in a vacuum desiccator for ∼45 min, after which it was poured into the lens mold and baked at 75 °C for ∼2 h. Following curing, uncrosslinked material in the lenses was extracted with toluene in a Soxhlet apparatus for ∼2 days. Lenses were then allowed to dry in air for at least 2 days before further treatment. The average value of R following these treatment steps was 4.84 ± 0.02 mm as determined from side-on images taken using a contact angle goniometer camera. Because R appeared to vary only minimally, its average value (and not an individually measured radius) was used in fitting the data for each sample.

Aqueous solutions of poly(allylamine hydrochloride) (PAH) ($M_w \approx 56\,000$ g/mol, Sigma-Aldrich) and poly(acrylic acid) (PAA)

(25% aqueous solution, M_w > 200 000 g/mol, Polysciences) were prepared at a concentration of 0.01 mol/L by repeat unit, and adjusted to pH 2.5 using 1 mol/L hydrochloric acid (HCl). Milli-Q deionized water (Millipore) with a resistivity >18 MΩ cm was used for all experimental purposes. Before LbL assembly, PDMS substrates were rinsed briefly with methanol and blown dry with nitrogen gas (N_2) to remove any dust from their surfaces. LbL coatings were constructed on PDMS by first immersing the substrates for 15 min in PAH, rinsing briefly in water, immersing the substrates for 15 min in PAA, and then rinsing again. These steps, which resulted in the formation of 1 bilayer, were repeated to create coatings with the desired thickness. After coatings were completed, they were gently blown dry with N_2. For in situ ellipsometry and X-ray photoelectron spectroscopy (XPS), coatings with 15.5 bilayers (LbL assembly began and ended in PAA solution) were constructed on silicon wafers that had been treated with 3-aminopropyltriethoxysilane (APTES) (Sigma-Aldrich) (see procedure below). Salt annealing was performed on the indicated samples by immersing them in 0.1 mol/L sodium chloride (NaCl) solutions for 1 h, followed by ~1 min of gentle rinsing in water.

Glass slides and silicon wafers to be treated with APTES were first washed in detergent and rinsed copiously with water. They were then treated for 20 min with UVO (Model 342, Jelight) and placed immediately into a 1 volume fraction (%) solution of APTES in anhydrous toluene (Sigma-Aldrich) for 1 h. After silanization, substrates were rinsed copiously with ethanol and toluene, blown dry with N_2, and baked overnight at 90 °C under a vacuum.

Aqueous 1×10^{-3} mol/L solutions of either NaCl or HCl were used as the pH 5.5 and 3.0 solutions described in this paper, respectively. A pH meter (Fisher Science Education) was used to determine the pH of solutions in this work to within ±0.1 pH units. Contact angles were measured using a DSA100 (Krüss) on APTES-glass and flat slabs of PDMS. Advancing images were taken seconds after pipeting 5 μL of solution manually onto the substrates. Another 5 μL of solution was pipetted onto the droplet, and after waiting ~20 min, a few microliters of solution were removed and a receding image was taken. The surface tension of 1×10^{-3} mol/L NaCl and HCl solutions was measured using the pendant drop technique. Values of 72.7 ± 0.3 mN/m and 71.7 ± 0.8 mN/m were obtained for NaCl and HCl solutions, respectively; these values were equal within error and very close to the expected value of ~72 mN/m for pure water at 25 °C (19).

Ellipsometry measurements were performed using an M-2000DI instrument (J.A. Woollam Co., Inc.) according to previously published methods (20). Uncertainty values for the LbL coating thicknesses were taken as one-half of the estimated surface roughness layer thickness as modeled in ambient air. The fits for 3 and 6 bilayer coatings on PDMS had an acceptable mean squared error (MSE) without inclusion of a surface roughness layer—for these samples, the uncertainty in the thickness was assumed to be 10%. In situ measurements were performed in a custom-built cell after 20 min of solution exposure; during modeling of the in situ data, the surface roughness was removed from the model for consistency in comparing the swelling of samples.

Sample staining was performed by immersing LbL-coated PDMS slabs or lenses into 1×10^{-3} mol/L solutions of methylene blue dye (MB) for 1 h, followed by a series of brief rinses in water (21). Absorption was measured using a spectrophotometer (PerkinElmer, Lambda 950), and spectra were normalized by subtracting the absorption of an uncoated PDMS substrate. The uncertainty in absorption measurements was assumed to be 10%. Absorption ratios were computed using the values obtained at 592 nm.

JKR adhesion experiments were performed using an axisymmetric design that consisted of an inverted microscope (Leica, DMIRE2), piezoelectric step motor (Burleigh, Inchworm IW-800), 10 g load cell (Futek, LSB200), and two optical distance sensors (Philtec, Inc., RC62). In a typical experiment, the lens was attached, facing downward, to a small piece of glass connected to the load cell/motor assembly via an ~2.5 cm aluminum rod. The circular contact region between the lens and a substrate secured on the sample holder of the inverted microscope was digitally photographed using a charge-coupled device (CCD) camera (Hamamatsu, ORCA-ER). Adhesion experiments were conducted by advancing the lens (at a speed of 1 μm/s) into the substrate in 2 μm steps, waiting 60 s between each step, until a maximum force of 0.5 g was reached. The lens was then pulled from the substrate using the same step/time settings, and the experiment was terminated when detachment occurred. All movement and measurement steps were automated using LabVIEW software (National Instruments). The load, distance, and image data were collected simultaneously at the end of each wait period. The radius of the circular contact area in each image was measured using Image Pro Plus (Media Cybernetics, Inc.). Example photographs are given in Figure S1 in the Supporting Information. Unless otherwise indicated, each JKR measurement was performed with a fresh, previously untested lens.

In situ adhesion experiments were performed in a cell that was custom-built using glass slides secured with optical adhesive and epoxy. After positioning the lens a few micrometers above the substrate, a solution of the desired pH was added and the system was allowed to equilibrate for 20 min before beginning a measurement.

The energy release rate (G) and the plane-strain Young's modulus (E^*) can be calculated by using the contact radius (a) in conjunction with either the load (P), vertical displacement (δ), or a combination of both latter parameters. Some authors have found using both P and δ leads to better fits of the data (6, 7); we found, however, that using both P and δ resulted in larger MSE values and non-normal distributions of E^*. Fitting a in conjunction with just P, on the other hand, led to lower MSE values, and resulted in normally distributed values of E^* with an average value of 2.3 MPa and a standard deviation of 0.3 MPa. Furthermore, these values of E^* obtained for the various lenses were representative of the bulk PDMS properties, as the presence or absence of LbL coatings did not appear to significantly affect the values of E^* obtained from the fits.

In light of the above considerations, we chose to use a P-only fit of eq 1 (least-squares algorithm). Both G_L and E^* were first obtained by fitting only the loading data to a linear form of eq 1

$$\frac{4a^{3/2}}{3R} = \frac{1}{E^*}\frac{P}{a^{3/2}} + \sqrt{\frac{8\pi G}{E^*}}. \qquad (2)$$

so that E^* could be found from the slope of the line, and G_L from the intercept (see Figure 1b). E^* was then held constant and the unloading data were fit to determine G_{UL}. In cases of strong adhesion, the first few unloading steps typically produce little to no change in the value of a. In these cases, a critical value of G must be reached before the contact circle radius begins to decrease (7). We thus only included a values that had decreased at least 1% from their maximum value in the unloading fit. We held E^* constant during the unloading fit for consistency in our experiments—in many cases, letting E^* (the inverse slope of the fitting line) take on a different value during unloading would have produced a better fit to the data (see Figure 1b), a fact observed by others as well (22). Nevertheless, E^* is a bulk lens property and hence there is no physical basis to let it change values during an experiment.

Atomic force microscopy (AFM) (Digital Instruments Dimension 3100 with a Nanoscope IV controller, Veeco Instruments)

was performed in tapping mode using silicon cantilevers. Arithmetic average roughness (R_a) was calculated using 5 μm $\times$ 5 μm images, except in one measurement of the APTES-glass surface for which a 1 μm $\times$ 1 μm image was used. The uncertainty in the roughness value for the annealed 6 bilayer surface was calculated from only two images, and thus represents the range of values measured. Only one measurement of the PDMS surface roughness was performed, and thus no uncertainty was available.

XPS was performed on samples as assembled and following salt annealing. Spectra were obtained on a Kratos AXIS Ultra DLD spectrometer using a monochromatic Al source. Atomic concentrations were calculated from survey spectra, collected over a binding-energy range from 1100 to 0 eV using a pass energy of 160 eV and a 100 ms dwell time. Three spectra were obtained at different locations for each sample. The elemental analysis results are given in detail in Table S1 in the Supporting Information.

There appeared to be significant variations in roughness between LbL-coated samples, especially for those taken from different batches; therefore, the samples used within a study to compare the affect of variables such as solution pH or surface roughness were always taken from the same batch. This batch-to-batch variability explains the difference in G_{HYS} measured in air for 3 and 6 bilayer coatings in Figures 4 and 5.

The relative humidity (RH) during all experiments conducted in laboratory air ranged from 40 to 50%, as measured using a digital humidity meter (Fisher Scientific). Unless otherwise indicated, uncertainty values given in this work represent one standard deviation calculated from at least three measurements.

RESULTS AND DISCUSSION

PDMS Adhesion to APTES-Glass. We first considered the adhesion behavior of uncoated PDMS lenses against APTES-glass. JKR adhesion experiments were conducted in air and in aqueous solutions of pH 3.0 and pH 5.5. Average G_{HYS} values are given in Figure 2.

Figure 2 illustrates that the adhesion between PDMS and APTES-glass is greatest when measured in air, with an average value of $G_{HYS} = 231 \pm 17$ mJ/m^2. The adhesion strength decreases in aqueous solution to a value of 101 ± 8 mJ/m^2 at pH 3.0 and 141 ± 5 mJ/m^2 at pH 5.5. This decrease in aqueous adhesion is in contrast to the findings of Chaudhury et al., who found increased adhesion between two hydrophobic (PDMS) surfaces in water (23). In our case, it is energetically favorable for water to partially wet the hydrophilic APTES-glass surface, competing with solid–solid wetting at the interface. Thus, in the absence of significant chemical bond formation, the wetting behavior of the interface controls whether systems will adhere better or worse when tested in water instead of air (24).

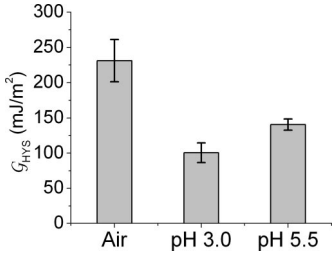

FIGURE 2. Adhesion hysteresis between PDMS and APTES-glass in air and in pH 3.0 and pH 5.5 aqueous solutions. The values of G_L and G_{UL} for this experiment are given in Figure S2 in the Supporting Information.

Table 1. Advancing and Receding Contact Angles of pH 3.0 and pH 5.5 Solutions on APTES-Glass and PDMS Surfaces

surface	solution pH	advancing contact angle (deg)	receding contact angle (deg)
APTES	3.0	63.0 ± 2.0	40.2 ± 3.5
	5.5	61.6 ± 3.8	41.8 ± 3.1
PDMS	3.0	103.8 ± 3.2	97.3 ± 0.3
	5.5	103.6 ± 3.9	93.8 ± 1.4

To better understand the dependence of PDMS adhesion on the solution pH, we performed contact angle measurements using pH 3.0 and 5.5 solutions. The results of these experiments are given in Table 1. Both APTES and PDMS surfaces exhibited some contact angle hysteresis, but the effect was much more pronounced for APTES, presumably because of charging and restructuring of the terminal amines. The contact angles measured using pH 3.0 and pH 5.5 solutions were identical within error, suggesting that ionization of the APTES-glass surface is insensitive to pH in this range. This result is expected as both solutions are well below the pK_a of APTES ($\approx$ 10) (19), and other studies have shown no change in the zeta potential of amine-functionalized particles between these pH values (25). PDMS, however, demonstrated slightly lower receding contact angles for pH 5.5 solution. Previous research has suggested that there should be no change in the adhesion properties of CH_3 functional groups as a function of pH (26). The difference that we observe is therefore probably due to ionization of residual silanol groups, which are known to be present in silicone polymers and can be created at their surface via hydrolysis (27). A change in silanol ionization has previously been observed for colloidal silica in this pH range (28)—the presence of these negatively charged groups at the PDMS surface could thus lead to acid–base interactions with amines upon contact with the APTES surface, increasing the adhesion hysteresis.

LbL-Coated PDMS Adhesion to APTES-Glass. LbL coatings were constructed on PDMS lenses via alternating deposition of PAH and PAA from solutions with adjusted pH values of 2.5. This particular system (hereafter PAH2.5/PAA2.5) was chosen because it is known to be rich in carboxylic acid functionality (29) and adsorbs well onto PDMS, exhibiting linear growth in thickness with the number of bilayers deposited (30). In addition, the two solution pH values chosen for in situ testing (pH 3.0 and pH 5.5) allowed us to tune the charge due to ionization of COOH groups at the lens surface, while still remaining below the pK_a of PAA ($\approx$ 6.5) (31) where the coating might swell substantially with possible compromised mechanical integrity. We chose to work with two thicknesses of LbL coating created by depositing either 3 or 6 bilayers of PAH2.5/PAA2.5 onto a PDMS lens. The thicknesses of these coatings were measured by performing ellipsometric measurements on flat slabs of PDMS that were coated with the same number of bilayers as the corresponding lenses. The ellipsometrically determined thicknesses were 15.9 ± 1.6 nm and 40 ± 4 nm for the 3 and 6 bilayer LbL coatings, respectively. These values

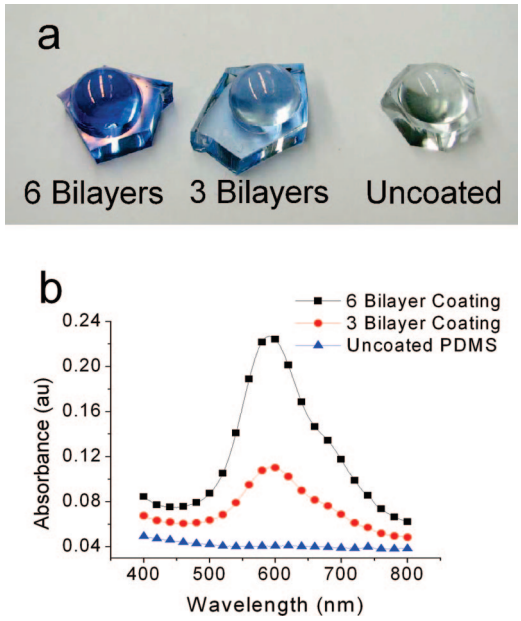

FIGURE 3. (a) Photograph of a 6 bilayer-coated, 3 bilayer-coated, and an uncoated PDMS lens after exposure to a MB dye solution for 1 h, followed by a brief rinse in water. (b) Absorbance spectra as measured on flat slabs of PDMS coated with the same systems shown in (a).

compare reasonably well with the average ≈ 5 nm/bilayer growth increment found in previous studies of the PAH2.5/PAA2.5 system (30). The relative thicknesses of the coatings were confirmed by staining the slabs in a solution of methylene blue (MB) dye, which has been shown to bind free acid groups in PAH/PAA coatings (21). Because the amount of acid groups available for binding scales with thickness, the relative intensity of the MB adsorption maxima from the samples reflects the coating thicknesses. A photograph of MB-stained, LbL-coated PDMS lenses and absorption spectra for the corresponding coating thicknesses are shown in images a and b in Figure 3, respectively. Figure 3 illustrates that while uncoated PDMS samples were not detectably stained with MB, LbL-coated PDMS lenses absorbed the dye in proportion to the thicknesses of the coatings. These coatings were conformal, and appeared visually uniform over the entire lens surface. The ratio of background-corrected maximum absorbance values for 6 and 3 bilayer coatings on flat slabs of PDMS was 2.7 ± 0.4, which agrees well with the ratio of thicknesses of 2.5 ± 0.4 obtained via ellipsometry.

JKR adhesion experiments for PDMS lenses having 3 and 6 bilayer coatings were conducted in air and in aqueous solutions of pH 3.0 and 5.5; the average values of G_{HYS} are given in Figure 4. LbL-coated lenses did not exhibit the comparatively large drop in G_{HYS} observed in Figure 2 for uncoated PDMS when the testing environment was changed from air to aqueous solution. In pH 5.5 solution the decrease in G_{HYS} was minimal, and at pH 3.0 G_{HYS} actually increased from the values measured in air. We note that the LbL coatings on the lenses tested in air were prepared in a different batch than the ones tested in aqueous solution, making it difficult to numerically compare the adhesion of the air- and aqueous-tested samples. Nevertheless, lack of a clear decrease in adhesion in moving to aqueous solutions is expected since the plasticization of the LbL in water (20) should allow COOH groups more mobility to reorient and interact with amines at the APTES-glass surface. The same trend would not be expected for uncoated lenses—water does not significantly plasticize PDMS, which already has a low glass-transition temperature ($T_g \approx -125$ °C) (19) and hence an extremely mobile interface.

Plasticization of the coating does not, however, account for all of our observations. The purpose of coating the lenses was to add additional acidic functionality to their surfaces; nevertheless, the uncoated PDMS displayed higher adhesion strength to the APTES-glass under all of the environmental conditions that we explored. Furthermore, the trend in adhesion hysteresis of LbL-coated lenses as a function of pH is opposite of expected—at the higher pH value, more COOH groups should ionize, increasing the adhesion hysteresis (as was observed to a minor extent for uncoated PDMS). LbL-coated lenses, however, exhibited a lower G_{HYS} at pH 5.5. Clearly, additional factors beyond mere surface chemistry must govern the adhesion behavior of such coatings.

Mechanical Properties and Surface Roughness of LbL Coatings. We utilized surface wrinkling (32) to measure the Young's modulus of LbL coatings assembled on flat slabs of PDMS. This technique has been described in detail elsewhere and is well-suited for determining the Young's modulus of LbL coatings (20, 30, 33). Two separate coatings were prepared comprising 10 and 14 bilayers of the PAH2.5/PAA2.5 system (thicker coatings were used for the mechanical properties characterization to ease measurement of the thickness and wrinkling wavelength). The wrinkling wavelength of each sample was measured using an optical microscope in ambient air and in pH 3.0 and 5.5 solutions. Ellipsometry was performed directly on the 10 and 14 bilayer samples in air (20), yielding coating thicknesses of 48 ± 9 nm and 80 ± 11 nm, respectively. Because of substrate size constraints in the in situ ellipsometer cell, coatings assembled on PDMS could not be measured directly. The in situ swollen thickness values of the coatings was instead estimated by performing measurements on PAH2.5/PAA2.5 coatings that had been assembled onto Si wafers, and then assuming the same swelling percentage for the coatings on PDMS.

Surface wrinkling yielded a value of 5.0 ± 2.0 GPa for the plane-strain Young's modulus of the coatings in air at a RH of ~40%. This is in reasonable agreement with the 6.8 ± 0.8 GPa obtained previously for the PAH2.5/PAA2.5 system at 36% RH (30). The LbL coating was effectively plasticized by both pH 3.0 and 5.5 solutions, and the swelling of each system was nearly equivalent, with values of 15.8 and 16.4% obtained in pH 3.0 and 5.5 solutions, respectively. Despite nearly identical swelling ratios, the modulus at pH 5.5 (1.8 ± 0.8 GPa) was more than double the value of 0.7 ± 0.2 GPa measured in pH 3.0 solution. These results would seem to confirm the existence of a strong hydrogen bonding (H-bonding) network in this system at pH values below the pK_a (≈ 6.5) of PAA; H-bonding has similarly been proposed

as an explanation for this system's resistance to swelling at low (<50%) relative humidity in air (30). The lack of a measurable difference in swelling of our coatings at pH 3.0 and 5.5 suggests that COOH ionization between pH 3.0 and 5.5 is not sufficient to induce large-scale disruption of H-bonding. The higher pH could, however, permit rearrangements of the chains on a much shorter time scale, allowing the system to adopt a more stable configuration, perhaps including the formation of additional electrostatic cross-links. These effects could lead to the observed increase in modulus.

We note that plane-strain Young's modulus values on the order of GPa for the PAH2.5/PAA2.5 system are surprising considering that exposing the same system to high humidity in air results in 3 times as much swelling and a modulus approximately an order of magnitude lower than we observed in pH 5.5 aqueous solution (30). Although it is possible that the internal interactions within the LbL coating could differ dependent upon whether the water was introduced in a vapor or a liquid state, nanoindentation experiments have measured Young's modulus values 5 orders of magnitude lower than our numbers for a similar system (PAH2.0/PAA2.0) in aqueous solution (34, 35). Another possible explanation is that our measured modulus values could possibly reflect a nonequilibrium state, as they were taken after only 20 min of equilibration in solution (as opposed to ~1 day for the humidity-controlled measurements) (30). Indeed, Tanchak et al. have reported that the PAH/PAA system assembled at low pH can have significantly extended equilibration times for swelling in slightly acidic solution (36). Further study is needed in order to definitively address these questions. In any case, we can suggest a possible mechanism for the adhesion behavior of the coated lenses based on our observation that the LbL assemblies retain a relatively high, pH-tunable modulus in solution.

JKR mechanics assumes contact between idealized, perfectly flat surfaces. According to this theory, E^* and G are independent constants, and the lens stiffness should not affect the measured adhesion. Fuller and Tabor, however, showed that materials contacting at rough interfaces exhibited decreases in G that were roughly proportional to both E^* and the arithmetic average roughness (R_a) (37). The explanation for this effect is due to the extra energy needed to deform height asperities in order to create interfacial contact when one or both surfaces are not perfectly smooth. While the ultrathin LbL coatings did not noticeably affect the bulk lens modulus ($E^* = 2.3 \pm 0.3$ MPa) obtained from fitting the adhesion data to the JKR equation (see the Experimental Section), they did result in a significant increase in stiffness in the near-surface region, as demonstrated through the wrinkling measurements. AFM measurements confirmed that the coatings also increased the lens surface roughness, with R_a values of 2.6 ± 0.7 nm and 10.4 ± 1.3 nm for 3 and 6 bilayer coatings, respectively, versus 0.54 nm for the bare PDMS surface and 0.65 ± 0.42 nm for APTES-glass. These data allow us to draw a comprehensive

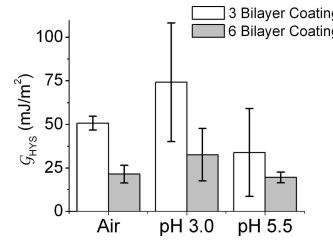

FIGURE 4. Adhesion hysteresis between LbL-coated PDMS and APTES-glass in air and in pH 3.0 and pH 5.5 aqueous solutions. Coatings comprising 3 bilayers and 6 bilayers were tested. The values of G_L and G_{UL} for this experiment are given in Figure S3 in the Supporting Information.

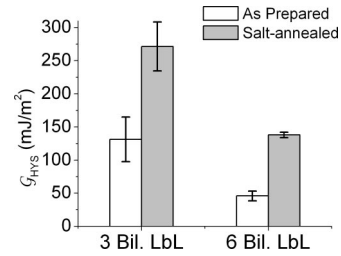

FIGURE 5. Effect of salt annealing on LbL-coated PDMS adhesion. The adhesion hysteresis for 3 bilayer and 6 bilayer coatings to APTES-glass in air for samples "as prepared", and samples that had been annealed for ~1 h in 0.1 mol/L NaCl. The values of G_L and G_{UL} for this experiment are given in Figure S4 in the Supporting Information. These measurements were performed on samples taken from a different batch than those presented in Figure 4, and had a higher average value of G_{HYS} for tests in air.

picture of the factors governing the adhesion of LbL-coated PDMS to APTES-glass.

LbL-coated lenses were expected to have a higher G_{HYS} than uncoated lenses due to favorable acid–base interactions with the APTES-glass substrate. Instead, coated lenses exhibited lower adhesion due to the comparatively higher roughness and stiffness of the LbL surface; these factors acted to decrease the area of intimate contact at the lens–substrate interface. For LbL-coated lenses in solution, increasing the solution pH to 5.5 should have increased the number of possible acid–base interactions at the interface through ionization of COOH groups, but instead resulted in decreased adhesion due to an approximately 2-fold increase in the LbL coating Young's modulus. Because of the presence of surface roughness, this modulus increase led to a decrease in adhesion for reasons explained previously. Finally, the effect of roughness on adhesion was made evident in the comparison of 3 and 6 bilayer coatings; the increased roughness of the latter system invariably led to lower adhesion measurements than the 3 bilayer coating when tested under the same conditions (see Figure 4). Our data also suggest that increased surface roughness led to higher uncertainty in the average adhesion hysteresis, as evidenced by the comparatively large error bars observed in the data for coated lenses (Figure 4) versus that observed for bare PDMS (Figure 2). ANOVA tests revealed that the decrease in statistical confidence levels of differences between G_{HYS} measured at pH 3.0 and pH 5.5 corresponds directly to an increase in the average roughness of the lens surface. The confidence levels for the uncoated, 3 bilayer-coated, and 6 bilayer-coated systems were 98, 93, and 86%, respectively.

Table 2. Average Arithmetic Average Roughness (R_a) As Determined by AFM for Surfaces Used in This Study; for LbL Surfaces, Values Are Given before and after Annealing the Coatings in 0.1 mol/L NaCl

system	R_a (nm) as prepared	R_a (nm) salt-annealed
PDMS	0.54	
APTES-glass	0.65 ± 0.42	
LbL-coated PDMS (3 bil.)	2.6 ± 0.7	1.4 ± 0.5
LbL-coated PDMS (6 bil.)	10.4 ± 1.3	6.2 ± 3.5

Other researchers have similarly reported that the modulus of LbL assemblies can significantly affect the adhesion behavior of these systems. Gong et al. found that the softer of two LbL coatings with positively charged PAH in the outermost layer adhered more strongly to negatively charged silica (38). Notley et al., who examined adhesion in a "symmetrical" system (contacting LbL coatings had outer layers of the same charge), also found stronger adhesion for coatings with less rigidity as determined using a quartz crystal microbalance (39).

Our measurements of LbL adhesion as a function of solution pH appear to be without literature precedence. Self-assembled monolayers with COOH functionality have shown clearly explainable trends in adhesion with pH (26), but these experiments were not designed to address surface roughness or modulus effects. Mermut et al. examined changes in adhesion for LbL coatings assembled at different pH values, thus reflecting different degrees of internal ionic cross-linking (40). They found higher adhesion for more tightly cross-linked systems, but the estimated Young's moduli for their systems were approximately 3 orders of magnitude lower than our coatings, making direct comparisons difficult.

Effects of Aqueous Salt Annealing. In order to test whether roughness governs adhesion in our LbL-coated PDMS system, we sought to smooth the coating surfaces before measurement. Previous authors have reported that immersing LbL assemblies in salt solutions can impart mobility to the chains that results in surface smoothing (salt annealing) (41), although partial or total dissolution can also take place (42, 43). Thus, the particular salt concentration needs to be selected carefully. Annealing the PAH2.5/PAA2.5 coatings in 0.1 mol/L NaCl solution for ~1 h decreased the roughness by approximately one-half, concomitant with an ~40% reduction in thickness in both samples. The relative fraction of coating thickness lost as measured by MB absorbance was equal for both the 3 and 6 bilayer coatings, a phenomenon consistent with previous reports (43). The pre- and post-annealing surface roughness (R_a) values for 3 and 6 bilayer LbL coatings on PDMS are presented in Table 2. The values of R_a obtained for uncoated PDMS and APTES-glass are also given for comparison.

To test the effects of the roughness reduction due to salt annealing on the adhesion of LbL-coated PDMS, we prepared a new batch of PAH2.5/PAA2.5 coated PDMS lenses, and the adhesion of 3 and 6 bilayer-coated lenses was measured for both "as-prepared" coatings, and coatings that had been annealed in NaCl solution. Adhesion experiments were conducted in air where the modulus of the coatings was highest and thus the effect of roughness would be most pronounced. The average values of G_{HYS} from these experiments are given in Figure 5.

Figure 5 demonstrates that salt annealing substantially increased the adhesion of LbL-coated lenses, with the highest value of G_{HYS} (270 ± 20 mJ/m^2) observed for the coating with the lowest surface roughness (3 bilayer salt-annealed coating, $R_a \approx 1$ nm), and the lowest value of G_{HYS} (46 ± 4 mJ/m^2) observed for the coating with the highest roughness (6 bilayer as prepared, $R_a \approx 10$ nm). The 3 bilayer coating as prepared and the salt-annealed 6 bilayer coating both had $G_{HYS} \approx 130$ mJ/m^2; the average roughness of the latter coating was higher, but still within error of the 3 bilayer system. Finally, we note that G_{HYS} value of 270 ± 20 mJ/m^2 obtained for the salt-annealed 3 bilayer coating—even with a R_a of 1.4 nm and a modulus on the order of several GPa—was still greater than the 231 ± 17 mJ/m^2 obtained for the smoother, uncoated PDMS lens (Figure 2). This finding is reassuring, and confirms that smooth LbL-coated lenses do indeed exhibit increased adhesion to APTES-glass. We performed XPS analysis of LbL coatings both as assembled and following salt annealing to ensure that the annealing step does not induce a change in surface chemistry that could provide an alternate explanation for the large increase in adhesion. The XPS data (see Table S1 in the the Supporting Information) indicated that the relative number of free carboxylic acid groups near the coating surface remained largely unchanged, although ~14% appeared to exchange their protons for sodium cations during the annealing step. Because this represents a small fraction of the free acids near the coating surface, it is unlikely to be the source of the large increase in adhesion upon NaCl annealing and instead indicates that the combined effects of the high modulus and surface roughness of LbL coatings are capable of masking strong adhesion interactions for all but the smoothest surfaces.

CONCLUSIONS

We have measured adhesion interactions between carboxylic acid-containing LbL coatings on PDMS and glass substrates functionalized with aminosilanes. Despite the increase in acid–base interactions expected with LbL functionalization, the coated lenses exhibited lower adhesion hysteresis than uncoated lenses in air and in pH 3.0 and pH 5.5 solutions. This was shown to be due to a combination of surface roughness and high coating modulus, which prevented the interface from establishing intimate contact. LbL coatings were effectively plasticized by aqueous solutions but to different degrees. The modulus of LbL coatings at pH 5.5 (1.8 ± 0.8 GPa) was approximately double the value of 0.7 ± 0.2 GPa measured in pH 3.0 solution, with the result that at pH 5.5, coated lenses displayed a lower adhesion hysteresis, even though the number of acid–base interactions should have been more numerous. By annealing LbL-coated lenses in low concentration NaCl solutions, the surface roughness was reduced and the adhesion increased significantly.

In this study, we have attempted to investigate the relative contribution of various LbL assembly properties to the in situ adhesion behavior of the coated surface. We have not, however, investigated the adhesion behavior of the coating itself to PDMS, although we note that the ability of the PAH2.5/PAA2.5 system to sustain the wrinkling instability (used for modulus measurements) suggests that adhesion at the PDMS-coating interface is strong. We have conducted some preliminary adhesion tests using the same lens to repeatedly contact fresh areas of the substrate up to five times—these results suggest that there is some small variation in adhesion with repeated tests, especially for 6 bilayer-coated lenses. Although there is no clear transition to PDMS-like adhesion as would be expected for complete coating removal, repeated testing could lead to changes in the coating roughness or partial transfer of polyelectrolyte multilayers from the coated lens to the APTES-glass substrate. These topics are important areas for future study.

The ability to measure and control adhesion is a topic of considerable technological importance. LbL assembly offers the ability to flexibly control surface composition but may introduce nontrivial changes to the interfacial properties that can influence the expected adhesion response. This work demonstrates how subtle, environmentally mediated changes in both the modulus and surface roughness can govern the adhesion response of an LbL coating; however, our results should be broadly applicable to understanding and controlling surface interactions in any system where adhesion is a matter of importance.

Acknowledgment. The authors thank Jing Zhou of NIST for experimental assistance, Aaron M. Forster and Nadia J. Edwin of NIST for careful reading of the manuscript, and Jenny A. Lichter of MIT for helpful discussions. A.J.N. acknowledges the NIST/National Research Council Postdoctoral Fellowship Program for funding.

Supporting Information Available: Optical micrographs of lenses contacting the APTES-glass substrate, loading and unloading energy release rates, and XPS data of LbL coatings as assembled and following salt annealing (PDF). This material is available free of charge via the Internet at http://pubs.acs.org.

REFERENCES AND NOTES

(1) Hong, Y. T.; He, Z. Q.; Lennhoff, N. S.; Banach, D. A.; Kanicki, J. *J. Electron. Mater.* **2004**, *33*, 312–320.
(2) Taylor, M.; Urquhart, A. J.; Anderson, D. G.; Williams, P. M.; Langer, R.; Alexander, M. R.; Davies, M. C. *Macromol. Rapid Commun.* **2008**, *29*, 1298–1302.
(3) Cappella, B.; Dietler, G. *Surf. Sci. Rep.* **1999**, *34*, 1–104.
(4) Israelachvili, J. N.; McGuiggan, P. M. *J. Mater. Res.* **1990**, *5*, 2223–2231.
(5) Johnson, K. L.; Kendall, K.; Roberts, A. D. *Proc. R. Soc. London, Ser. A* **1971**, *324*, 301–313.
(6) Chin, P.; McCullough, R. L.; Wu, W. L. *J. Adhes.* **1997**, *64*, 145–160.
(7) Shull, K. R. *Mater. Sci. Eng., R* **2002**, *36*, 1–45.
(8) Dillow, A. K.; Ochsenhirt, S. E.; McCarthy, J. B.; Fields, G. B.; Tirrell, M. *Biomaterials* **2001**, *22*, 1493–1505.
(9) Huang, H.; Chung, J. Y.; Nolte, A. J.; Stafford, C. M. *Chem. Mater.* **2007**, *19*, 6555–6560.
(10) La Spina, R.; Tomlinson, M. R.; Ruiz-Perez, L.; Chiche, A.; Langridge, S.; Geoghegan, M. *Angew. Chem., Int. Ed.* **2007**, *46*, 6460–6463.
(11) Chu, Y. S.; Dufour, S.; Thiery, J. P.; Perez, E.; Pincet, F. *Phys. Rev. Lett.* **2005**, *94*, 028102.
(12) Elsner, N.; Dubreuil, F.; Fery, A. *Phys. Rev. E* **2004**, *69*, 031802.
(13) Nam, J.; Santore, M. M. *Langmuir* **2007**, *23*, 10650–10660.
(14) Rundlöf, M.; Karlsson, M.; Wågberg, L.; Poptoshev, E.; Rutland, M.; Claesson, P. *J. Colloid Interface Sci.* **2000**, *230*, 441–447.
(15) Lee, D.; Rubner, M. F.; Cohen, R. E. *Nano Lett.* **2006**, *6*, 2305–2312.
(16) Lvov, Y.; Ariga, K.; Ichinose, I.; Kunitake, T. *J. Am. Chem. Soc.* **1995**, *117*, 6117–6123.
(17) Lvov, Y.; Decher, G.; Sukhorukov, G. *Macromolecules* **1993**, *26*, 5396–5399.
(18) Decher, G. *Science* **1997**, *277*, 1232–1237.
(19) Lide, D. R., *CRC Handbook of Chemistry and Physics*, 88th ed.; CRC Press/Taylor and Francis: Boca Raton, FL, 2007.
(20) Nolte, A. J.; Rubner, M. F.; Cohen, R. E. *Macromolecules* **2005**, *38*, 5367–5370.
(21) Chung, A. J.; Rubner, M. F. *Langmuir* **2002**, *18*, 1176–1183.
(22) Silberzan, P.; Perutz, S.; Kramer, E. J.; Chaudhury, M. K. *Langmuir* **1994**, *10*, 2466–2470.
(23) Chaudhury, M. K.; Whitesides, G. M. *Langmuir* **1991**, *7*, 1013–1025.
(24) Lingström, R.; Notley, S. M.; Wågberg, L. *J. Colloid Interface Sci.* **2007**, *314*, 1–9.
(25) Lee, D.; Gemici, Z.; Rubner, M. F.; Cohen, R. E. *Langmuir* **2007**, *23*, 8833–8837.
(26) van der Vegte, E. W.; Hadziioannou, G. *J. Phys. Chem. B* **1997**, *101*, 9563–9569.
(27) Gent, A. N.; Vondráček, P. *J. Appl. Polym. Sci.* **1982**, *27*, 4357–4364.
(28) Iler, R. K. *The Chemistry of Silica*; John Wiley & Sons: New York, 1979.
(29) Shiratori, S. S.; Rubner, M. F. *Macromolecules* **2000**, *33*, 4213–4219.
(30) Nolte, A. J.; Treat, N. D.; Cohen, R. E.; Rubner, M. F. *Macromolecules* **2008**, *41*, 5793–5798.
(31) Choi, J.; Rubner, M. F. *Macromolecules* **2005**, *38*, 116–124.
(32) Stafford, C. M.; Harrison, C.; Beers, K. L.; Karim, A.; Amis, E. J.; Vanlandingham, M. R.; Kim, H. C.; Volksen, W.; Miller, R. D.; Simonyi, E. E. *Nat. Mater.* **2004**, *3*, 545–550.
(33) Nolte, A. J.; Cohen, R. E.; Rubner, M. F. *Macromolecules* **2006**, *39*, 4841–4847.
(34) Thompson, M. T.; Berg, M. C.; Tobias, I. S.; Rubner, M. F.; Van Vliet, K. J. *Biomaterials* **2005**, *26*, 6836–6845.
(35) Lichter, J. A.; Thompson, M. T.; Delgadillo, M.; Nishikawa, T.; Rubner, M. F.; Van Vliet, K. J. *Biomacromolecules* **2008**, *9*, 1571–1578.
(36) Tanchak, O. M.; Barrett, C. J. *Chem. Mater.* **2004**, *16*, 2734–2739.
(37) Fuller, K. N. G.; Tabor, D. *Proc. R. Soc. London, Ser. A* **1975**, *345*, 327–342.
(38) Gong, H. F.; Garcia-Turiel, J.; Vasilev, K.; Vinogradova, O. I. *Langmuir* **2005**, *21*, 7545–7550.
(39) Notley, S. M.; Eriksson, M.; Wågberg, L. *J. Colloid Interface Sci.* **2005**, *292*, 29–37.
(40) Mermut, O.; Lefebvre, J.; Gray, D. G.; Barrett, C. J. *Macromolecules* **2003**, *36*, 8819–8824.
(41) Dubas, S. T.; Schlenoff, J. B. *Langmuir* **2001**, *17*, 7725–7727.
(42) Lynn, D. M. *Adv. Mater.* **2007**, *19*, 4118–4130.
(43) Nolte, A. J.; Takane, N.; Hindman, E.; Gaynor, W.; Rubner, M. F.; Cohen, R. E. *Macromolecules* **2007**, *40*, 5479–5486.

AM8000874